Asymmetry in pulsed four-wave mixing

H. Friedmann and A. D. Wilson-Gordon
Department of Chemistry, Bar-Ilan University, Ramat Gan 52900, Israel
(Received 15 October 1996; revised manuscript received 14 October 1997)

The Bloch equations are solved for a two-level system interacting with a strong pulsed laser pump and a weak pulsed laser probe. It is shown that the four-wave-mixing excitation spectrum, which is symmetrical with respect to the pump-probe detuning δ in the steady-state regime, becomes asymmetrical under pulsed conditions. The asymmetry is ascribed mainly to the linewidths of the pump and probe laser pulses. [S1050-2947(98)02306-3]

PACS number(s): 42.65.Hw, 42.50.Md, 42.65.Vh

I. INTRODUCTION

The four-wave-mixing (FWM) signal at frequency $2\omega_1 - \omega_2$, obtained by the interaction of a two-level system with a weak probe of varying frequency ω_2 and a pump of arbitrary intensity and fixed frequency ω_1, has been studied in detail by Boyd and co-workers [1] in the steady-state regime. In the presence of collisions, a symmetrical three-peaked spectrum is obtained for the FWM excitation spectrum. The strong, extraresonant peak, observed by Bogdan *et al.* [2], occupies the central position at

$$\omega_2 = \omega_1 . \tag{1}$$

The weaker Rabi sidebands are situated at

$$\omega_2 = \omega_1 \pm \Omega_1 = \omega_1 \pm (\Delta_1^2 + 4|V_1^2|)^{1/2}, \tag{2}$$

where $2V_1$ and Ω_1 are the pump Rabi and generalized Rabi frequencies and

$$\Delta_1 = \omega_{ba} - \omega_1 \tag{3}$$

is the detuning of the pump laser from resonance.

In a previous publication [3], we extended the calculations of Boyd and co-workers [1] to the case where the probe intensity also becomes arbitrarily large. We found that with increasing probe intensity, the Rabi sideband situated near ω_{ba} gradually becomes weaker than the other sideband, situated near the three-photon scattering (TPS) frequency $2\omega_1 - \omega_{ba}$. The weakness of the sideband at $\omega_2 \approx \omega_{ba}$ was shown to arise from saturation of the two-level system. The resulting asymmetry of the FWM excitation spectrum was recently observed by Chalupczak, Gawlik, and Zachorowski [4] at high probe intensity [see Fig. 7(b) of Ref. [4]]. However, at low probe intensity, the opposite asymmetry, in favor of the Rabi sideband near the resonance frequency [see Fig. 7(a) of Ref. [4]], was obtained. This result contradicts the theoretical predictions [1,3].

We believe that the discrepancy between theory and experiment arises from the fact that the steady-state analysis of FWM is inadequate for the description of the experiments of Chalupczak *et al.* where pulsed lasers were used. We shall show in the subsequent sections that, under pulsed conditions, the nonstationary time-dependent solutions of the Bloch equations can lead to asymmetry in the FWM spectrum in the case of a weak probe.

In order to explain the effect, we have tried to reduce the complexity of the system by omitting collisions and taking pump-pulse parameters that obey adiabatic following conditions. The asymmetry then depends mainly on the linewidth of the probe laser pulse and that of the pump laser.

II. THEORY

Consider a two-level system interacting with a bichromatic field

$$\vec{E}(t) = \tfrac{1}{2}\vec{\varepsilon}[E_1(t) + E_2(t)\exp(-i\delta t)]\exp(-i\omega_1 t) + \text{c.c.}, \tag{4}$$

where ω_1 and $\omega_2 = \omega_1 + \delta$ are the frequencies of the strong pump field with a time-dependent electric-field strength $E_1(t)$ and of the weak probe with electric-field strength $E_2(t)$. Denoting the time-dependent Rabi frequencies by

$$2V_1(t) = \mu_{ab}E_1(t)/\hbar, \quad 2V_2(t) = \mu_{ab}E_2(t)/\hbar, \tag{5}$$

we write the Bloch equations in the rotating-wave approximation as [1,5,6]

$$i\dot{\rho}_{ab} = -(\omega_{ba} + i/T_2)\rho_{ab} - [V_1^*(t) + V_2^*(t)e^{i\delta t}] \times e^{i\omega_1 t}(\rho_{bb} - \rho_{aa}) \tag{6}$$

and

$$(\dot{\rho}_{bb} - \dot{\rho}_{aa}) = -4\,\mathrm{Im}\{[V_1(t) + V_2(t)e^{-i\delta t}]e^{-i\omega_1 t}\rho_{ab}\} - (1/T_1)(\rho_{bb} - \rho_{aa}) - 1/T_1 . \tag{7}$$

We now write the density matrix in the form

$$\rho = \rho^0 + \Delta\rho, \tag{8}$$

where ρ^0 is the solution of Eqs. (6) and (7) when $V_2 = 0$. Writing the matrix elements of ρ^0 as

$$\rho_{ba}^0 = \rho_{ba}(\omega_1)e^{-i\omega_1 t} = (\rho_{ab}^0)^* = \rho_{ab}(-\omega_1)e^{i\omega_1 t} \tag{9}$$

and $(\rho_{bb} - \rho_{aa})^0$, it follows from Eqs. (6) and (7) that

$$i\dot{\rho}_{ab}(-\omega_1)=-(\Delta_1+i/T_2)\rho_{ab}(-\omega_1)-V_1^*(t)(\rho_{bb}-\rho_{aa})^0 \tag{10}$$

and

$$(\dot{\rho}_{bb}-\dot{\rho}_{aa})^0=-4\,\mathrm{Im}[V_1(t)\rho_{ab}(-\omega_1)]-(1/T_1)(\rho_{bb}-\rho_{aa})^0 -1/T_1. \tag{11}$$

Inserting Eq. (8) into Eqs. (6) and (7) and using Eqs. (9)–(11), we find to first order in the probe Rabi frequency V_2 and to all orders in V_1 that

$$\Delta\rho_{ba}=\rho_{ba}(\omega_2)e^{-i\omega_1 t}e^{-i\delta t}+\rho_{ba}(2\omega_1-\omega_2)e^{-i\omega_1 t}e^{i\delta t} =\Delta\rho_{ab}^* \tag{12}$$

and

$$\Delta\rho_{bb}-\Delta\rho_{aa}=(\rho_{bb}-\rho_{aa})^{(\delta)}e^{-i\delta t}+(\rho_{bb}-\rho_{aa})^{(-\delta)}e^{i\delta t}, \tag{13}$$

where $(\rho_{bb}-\rho_{aa})^{(\pm\delta)}$ are the population-pulsation Fourier components defined in Eq. (12) of Ref. [1]. Since $\Delta\rho_{bb}-\Delta\rho_{aa}$ is real,

$$(\rho_{bb}-\rho_{aa})^{(\delta)}=[(\rho_{bb}-\rho_{aa})^{(-\delta)}]^*. \tag{14}$$

We also find that the Fourier components $\rho_{ba}(\omega_2)$, $\rho_{ab}(\omega_2-2\omega_1)$, and $(\rho_{bb}-\rho_{aa})^{(\delta)}$ of Eqs. (12)–(14) satisfy the Bloch equations (compare [6])

$$i\dot{\rho}_{ba}(\omega_2)=(\Delta_1-\delta-i/T_2)\rho_{ba}(\omega_2)+V_1(t)(\rho_{bb}-\rho_{aa})^{(\delta)} +V_2(t)(\rho_{bb}-\rho_{aa})^0, \tag{15}$$

$$i\dot{\rho}_{ab}(\omega_2-2\omega_1)=-(\Delta_1+\delta+i/T_2)\rho_{ab}(\omega_2-2\omega_1) -V_1^*(t)(\rho_{bb}-\rho_{aa})^{(\delta)}, \tag{16}$$

$$i(\dot{\rho}_{bb}-\dot{\rho}_{aa})^{(\delta)}=-(\delta+i/T_1)(\rho_{bb}-\rho_{aa})^{(\delta)}+2V_1^*(t)\rho_{ba}(\omega_2) -2V_1(t)\rho_{ab}(\omega_2-2\omega_1) -2V_2(t)\rho_{ab}(-\omega_1). \tag{17}$$

Since $V_1(t)$ and $V_2(t)$ are time dependent, the Bloch equations (10), (11), and (15)–(17) must be solved numerically. This allows us to calculate $\rho_{ab}(\omega_2-2\omega_1)$ as a function of δ and time. In order to compare this result with the steady-state value of the FWM signal intensity, which is proportional to the square of the absolute value of $\rho_{ab}(\omega_2-2\omega_1)$ for a thin slab of two-level systems and depends only on δ, we integrate $|\rho_{ab}(\omega_2-2\omega_1)|^2$ over time

$$\langle|\rho_{ab}(\omega_2-2\omega_1)|^2\rangle=\int_{-\infty}^{+\infty}|\rho_{ab}(\omega_2-2\omega_1)|^2 d(t/T_2), \tag{18}$$

where, in order to obtain a dimensionless quantity, we use the transverse relaxation time T_2 as the unit of time.

The thin-slab approximation is considered here in order to account for the experimental setup of Chalupczak *et al.* [4] in which the probe beam, arriving at an angle, interacts only with a small portion of the pump beam. The FWM signal also leaves the pump beam at the phase-matching angle. In order to account for propagation, we must therefore multiply the thin-slab expression for the FWM process by $\exp(-\alpha L-\alpha' L')$, where α is the absorption coefficient of the probe and L its optical path in the linear region, whereas α' is the absorption coefficient of the outgoing FWM signal and L' its optical path in the linear region. Switching from one Rabi sideband to the other will interchange α and α' and so, by choosing $L=L'$, both bands will be equally affected by propagation. The difference between the two sidebands is then only due to the difference in value of $\rho_{ab}(\omega_2-2\omega_1)$ (see the next section). This conclusion is not modified qualitatively beyond the thin-slab approximation provided that propagation length in the nonlinear medium is much smaller than the diffraction length. Propagation will only amplify the effect since the amplification is also determined by $\rho_{ab}(\omega_2-2\omega_1)$ [1].

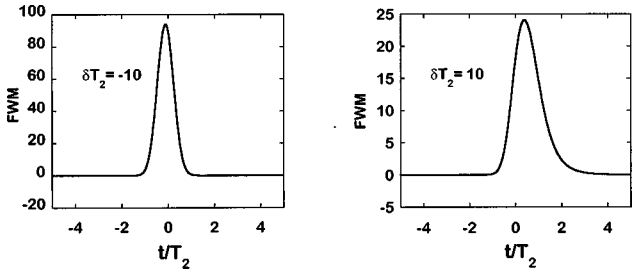

FIG. 1. Time-dependent four-wave-mixing excitation spectrum $[|\rho_{ab}(\omega_2-2\omega_1)|^2\times 10^7$ is plotted] for $\delta T_2=\pm 10$, $D_1=T_2$, $D_2=24T_2$, $T_1=3T_2$, $\Delta t_0=0$, and $\Delta_1 T_2=-10$. V_1 is defined as in Eq. (21) and $V_2=V_1/100$. Note that the plots do not change when Δt_0 is changed provided $\Delta t_0<D_2$.

III. RESULTS AND DISCUSSION

We have calculated the solutions of the Bloch equations using Gaussian-shaped pulses

$$V_1(t)=V_1\exp[-t^2/D_1^2], \tag{19}$$

$$V_2(t)=V_2\exp[-(t-\Delta t_0)^2/D_2^2], \tag{20}$$

where Δt_0 is the time delay between the pump and probe, $V_2\ll V_1$ ($V_2=V_1/100$), and V_1 is chosen such that

$$\int_{-\infty}^{\infty}2V_1(t)dt=2V_1\pi^{1/2}D_1=4\pi. \tag{21}$$

It should be noted that Eq. (21) does not represent a true 4π pulse in our numerical calculations since we take the pump to be detuned from resonance and its duration to be of the order of the transverse relaxation time T_2, as in the experiments of Chalupczak *et al.* [4]. These two factors smooth out the oscillations that would be produced by a true 4π pulse. For the detunings used in our calculations, we have verified that the pump laser never produces equal populations, let alone population inversion. This remains true when the bare atom states are replaced by the instantaneous, semiclassical dressed-atom states [7].

In Figs. 1 and 2 we have chosen $D_1=T_2$, $D_2=24T_2$, $T_1=3T_2$, $\Delta_1 T_2=-10$, and $\Delta t_0=0$. We see that both the time-

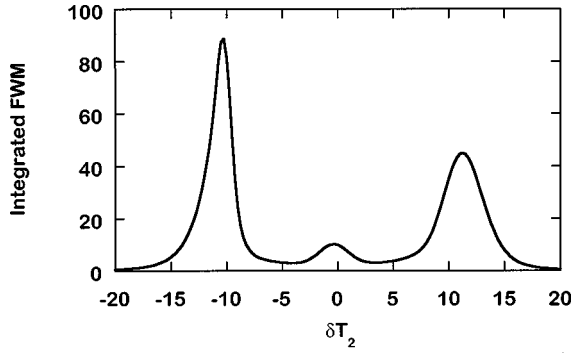

FIG. 2. Time-integrated four-wave-mixing excitation spectrum as a function of δT_2. (Parameters and scaling are the same as in Fig. 1.)

dependent values of $|\rho_{ab}(\omega_2-2\omega_1)|^2$ (Fig. 1) and its time-integrated values [see Eq. (18) and Fig. 2] are asymmetrical with respect to the transformation $\delta\rightarrow-\delta$ and that the asymmetry favors the Rabi sideband situated near the resonance frequency, where $\delta\simeq\Delta_1$ or $\omega_2\simeq\omega_{ba}$, over the Rabi sideband near the TPS frequency, where $\delta\simeq-\Delta_1$ or $\omega_2\simeq2\omega_1-\omega_{ba}$. This is in agreement with the experiment of Chalupczak *et al.* [4] mentioned in the Introduction. We have verified that this result is independent of Δt_0 (provided $\Delta t_0<D_2$). We have also found that the symmetrical steady-state situation is reestablished by increasing the pump width D_1. Clearly, the asymmetry is caused by the rapid time variation of the pump.

In Figs. 3 and 4 we have chosen $D_1=D_2=T_2$, $T_1=3T_2$, and $\Delta_1T_2=-10$. For this case, the relative intensity of the Rabi sidebands depends on the value of Δt_0. For $\Delta t_0=-0.4T_2$, the Rabi sideband near the resonance frequency is larger than that near the TPS frequency. However, for $\Delta t_0=0.4T_2$, the opposite result is obtained. Moreover, the Rabi sideband at the resonance frequency is now about three times weaker than in the case where $\Delta t_0=-0.4T_2$. There is little change in the intensity of the Rabi sideband near the TPS frequency in going from $\Delta t_0=-0.4T_2$ to $\Delta t_0=0.4T_2$.

In summary, we have established that under pulsed conditions, the FWM signal may be an asymmetric function of the pump-probe detuning δT_2 and of the pump-probe time delay Δt_0. The extent and direction of the asymmetry can be altered by changing experimental parameters such as the pump detuning from resonance, and the widths and intensities of the pump and probe pulses and the delay between them. We note that the asymmetry only occurs when D_1 is small, that is, when the pump field is strongly varying with time. Nevertheless, for the parameters used in Figs. 1–4, the adiabaticity conditions of Grischkowsky [8], Flusberg and Hartmann [9], and Eq. (3.35) of Allen and Eberly [10],

$$|\Delta_1|>1/D_1>1/T_1,1/T_2, \tag{22}$$

$$|2\Delta_1\dot{V}_1(t)|\ll[\Delta_1^2+4|V_1(t)|^2]^{3/2}, \tag{23}$$

do not hold. For these parameters, $1/D_1=1/T_2$ and thus the second inequality of Eq. (22) is not obeyed. Moreover, the left-hand side of the inequality of Eq. (23) can be as large as 5% of the right-hand side.

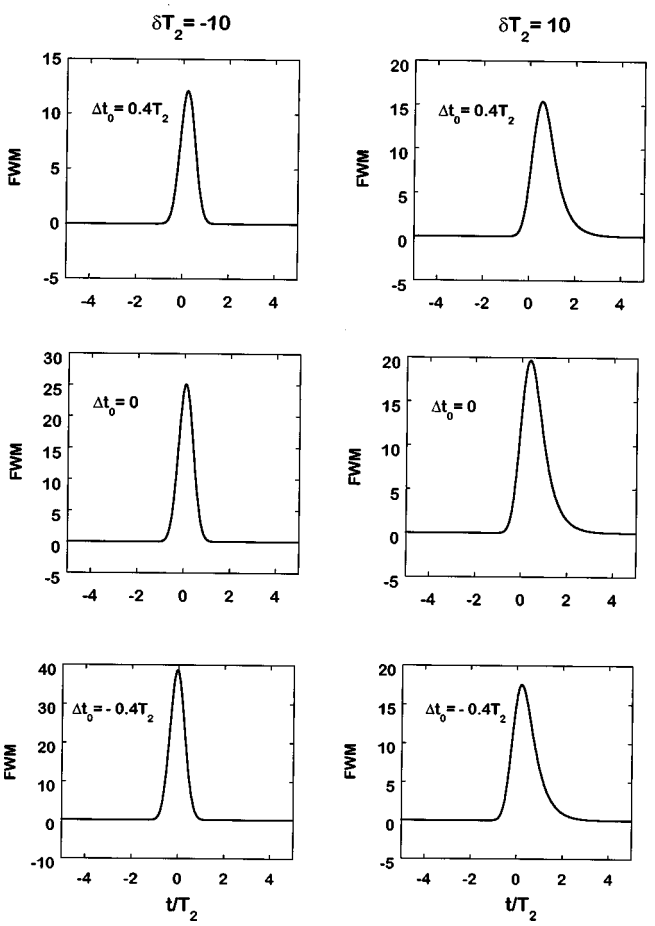

FIG. 3. Time-dependent four-wave-mixing excitation spectrum [$|\rho_{ab}(\omega_2-2\omega_1)|^2\times10^7$ is plotted] for $\delta T_2=\pm10$, $D_1=D_2=T_2$, $T_1=3T_2$, and $\Delta_1T_2=-10$ and for three values of the time delay Δt_0 between the pump and probe. Note that the asymmetry with respect to the transformation of δT_2 from -10 to 10 depends on the value of Δt_0. Similarly, we note that the asymmetry with respect to the transformation of Δt_0 from $-0.4T_2$ to $0.4T_2$ depends on the value of δT_2.

As we have seen, the parameters used above can lead to qualitative agreement with the results of Chalupczak *et al.* [4]. However, the system is too complex to allow physical insight into the fundamental cause of the difference between the symmetrical, steady-state FWM spectrum and the asymmetrical pulsed spectrum. In order to simplify matters, we omit collisions and take D_1 sufficiently small and Δ_1 sufficiently large so that the inequalities of Eqs. (22) and (23) are satisfied. We note that increasing the adiabaticity of the pump by increasing Δ_1 leads to a gradual reduction in the ratio of the intensity of the resonance sideband to that of the TPS sideband (see Fig. 5). However, even when adiabatic conditions are well obeyed there remains an asymmetry in both the peak intensity and width of the two sidebands. For such an adiabatic pulse, we varied the probe duration, with the following results (see Fig. 6): As long as D_2 is sufficiently large, the asymmetry in the peak intensity is in favor of the resonance Rabi sideband. However, this asymmetry is gradually inverted as D_2 decreases and, at the same time, the width of the resonance sideband increases.

There seems to be only one possible explanation for this effect. As long as the probe linewidth (proportional to $1/D_2$)

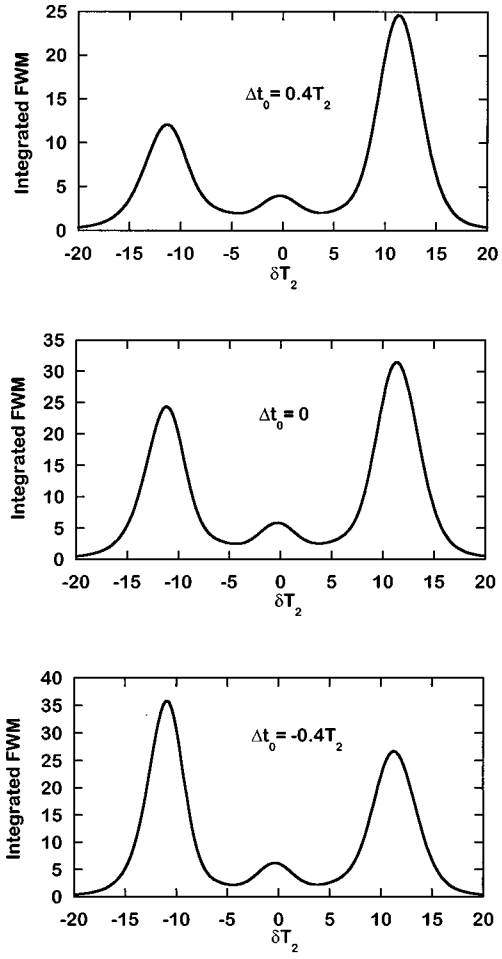

FIG. 4. Time-integrated four-wave-mixing excitation spectrum as a function of δT_2. (Parameters and scaling are the same as in Fig. 3.)

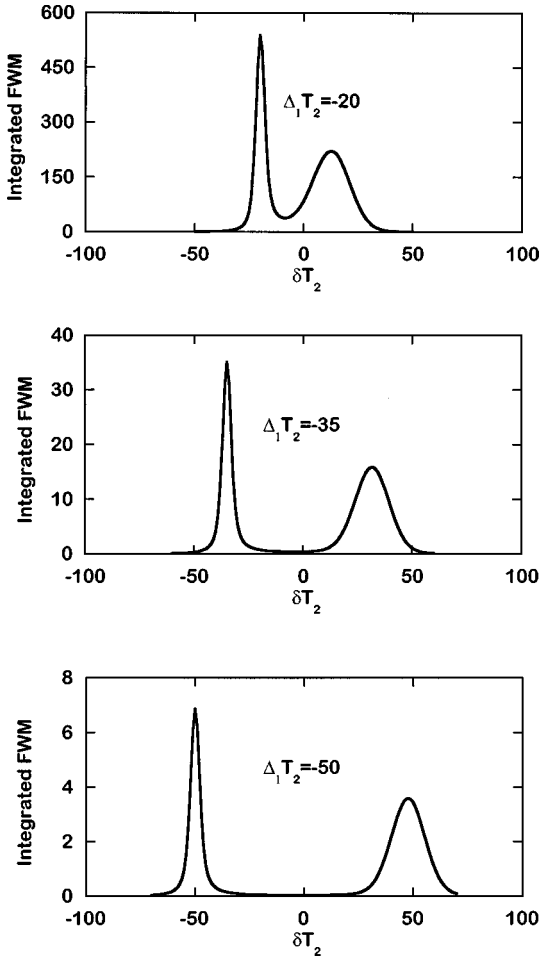

FIG. 5. Time-integrated four-wave-mixing excitation spectrum $[|\rho_{ab}(\omega_2 - 2\omega_1)|^2 \times 10^{15}$ is plotted] as a function of δT_2, for an adiabatic pump pulse for various values of the pump detuning. The parameters are $D_1 = 0.2T_2$, $D_2 = T_2$, $T_2 = 2T_1$, and pulse area 0.1π.

is small, there is good overlap between the probe linewidth and that of the $|b\rangle \rightarrow |a\rangle$ transition, when the probe laser is at the frequency of the resonance sideband. However, when the probe is at the frequency of the TPS sideband, the small probe linewidth produces inadequate overlap with the pump linewidth (proportional to $1/D_1$), which determines the TPS linewidth. This explains the asymmetry of the FWM excitation spectrum in favor of the resonance sideband. It also explains the difference in the width of the two sidebands. The situation is inverted when D_2 becomes small so that the probe linewidth overlaps with that of the pump but becomes much broader than the linewidth of the $|b\rangle \rightarrow |a\rangle$ transition. It is obvious that this explanation also accounts for the variation in the linewidths of the two sidebands, on varying D_2, and for the fact that the asymmetry disappears altogether when D_1 becomes large so that the only linewidth seen by the probe is the linewidth of the transition, namely, $1/T_2$. The present calculations are restricted to pulsed pump and probe lasers and describe transient effects. However, we have verified that similar FWM asymmetry effects can be obtained in the steady state where, for Lorentzian laser line shapes, laser linewidth effects are described by the replacement

$$\omega_{1,2} \rightarrow \omega_{1,2} + i\gamma_{1,2}. \tag{24}$$

Here $\gamma_{1,2}$ are the pump and probe linewidths [11]. For more sophisticated methods leading essentially to the same result, see Refs. [12,13]. Thus the symmetrical, steady-state FWM spectrum [1] is only due to the neglect of laser linewidth effects.

The modification of the time-integrated FWM excitation spectrum with respect to the transformation of the pump-probe time delay from $-\Delta t_0 \rightarrow \Delta t_0$, shown in Fig. 4, also survives when the pump laser obeys the adiabaticity conditions of Eqs. (22) and (23) (see Fig. 7). It is well known that, for short adiabatic pump pulses, the absorption depends not only on the pump detuning and intensity but also on dV_1/dt [see Eq. (3.44b) of Ref. [10]]. This is a group-velocity signature that arises whenever energy is stripped from the front of the pulse and returned to the back of the pulse, producing a group velocity smaller than c. Such behavior occurs not only in the adiabatic limit but is well known for nonadiabatic pulses that are nearly 2π and where the entire population is cycled through the excited state and back again (see p. 352 of Ref. [14]).

It is not clear why, in the adiabatic limit, the asymmetry induced by the sign of dV_1/dt should affect only the Rabi sideband at the resonance frequency (see Fig. 7). We believe that, although we have tried to eliminate pump nonadiabatic-

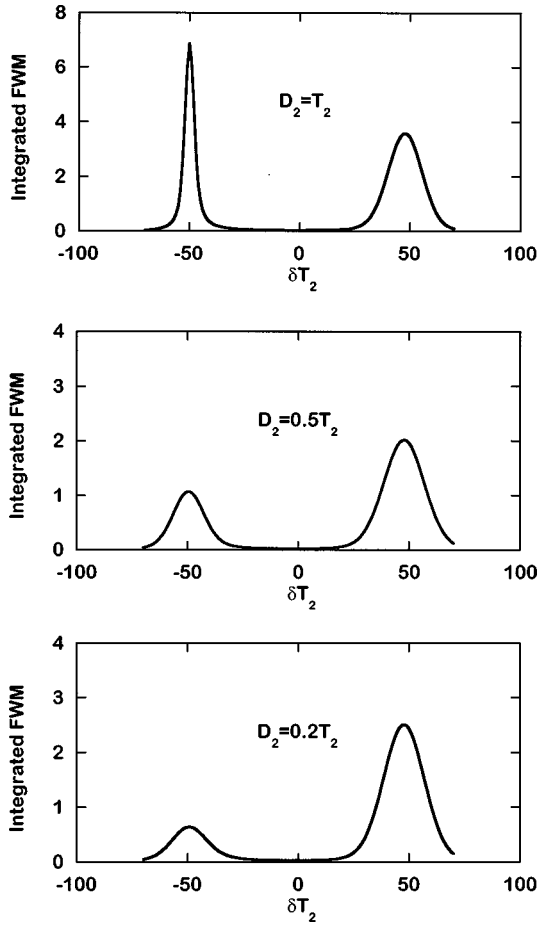

FIG. 6. Time-integrated four-wave-mixing excitation spectrum $[|\rho_{ab}(\omega_2-2\omega_1)|^2\times10^{15}$ is plotted] as a function of δT_2, for an adiabatic pump pulse for various values of D_2. The parameters are $D_1=0.2T_2$, $T_2=2T_1$, $\Delta_1T_2=-50$, and pulse area 0.1π.

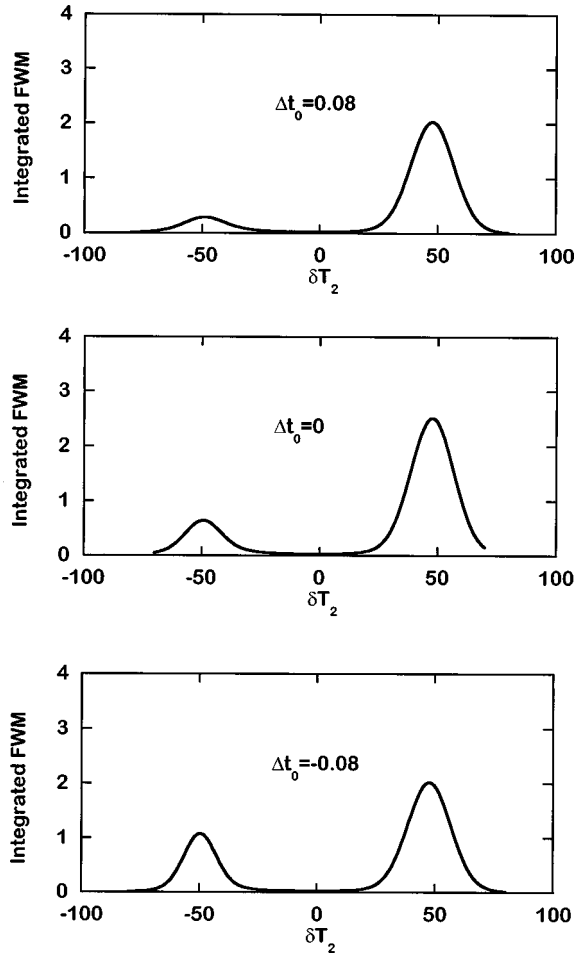

FIG. 7. Time-integrated four-wave-mixing excitation spectrum $[|\rho_{ab}(\omega_2-2\omega_1)|^2\times10^{15}$ is plotted] as a function of δT_2, for an adiabatic pump pulse for various values of Δt_0. The parameters are $D_1=D_2=0.2T_2$, $T_2=2T_1$, $\Delta_1T_2=-50$, and pulse area 0.1π.

ity by increasing the detuning Δ_1, a small, residual amount of nonadiabatic transitions is unavoidable. Since the FWM intensity also decreases very rapidly with increasing Δ_1, nonadiabatic pathways, such as the one depicted in Fig. 8, may give an important contribution in the case where the probe is at the resonance frequency, but not when it is at the nonresonant TPS frequency. Nonadiabaticity increases the occupation rate of the upper state $|b\rangle$ of the two-level system at the leading edge of the pump pulse, but reduces this occupation rate at the trailing edge. Therefore, only when Δt_0 is negative will this nonadiabaticity increase the probability of the $|b\rangle$ to $|a\rangle$ transition induced by a resonant probe laser, as required for the FWM process of Fig. 8. This can also explain the results of Fig. 5 where, although the adiabaticity conditions are well obeyed in the three cases depicted, still the ratio of the intensities of the resonance and TPS sidebands decreases slightly with increasing Δ_1, that is, with decreasing probability of nonadiabatic transitions induced by the pump pulse. Note also that adiabaticity cannot be restored in the near-resonance, large signal (large V_1, small Δ_1) regime as shown in the Appendix.

IV. CONCLUSION

A series of different effects are predicted in FWM spectra obtained with a nearly resonant pump and a weak probe, provided the pump spectral linewidth is larger than (or at least of the same order as) the linewidth of the atomic transition. Thus we predict that the FWM excitation spectrum will be asymmetrical: The intensity of the Rabi sideband

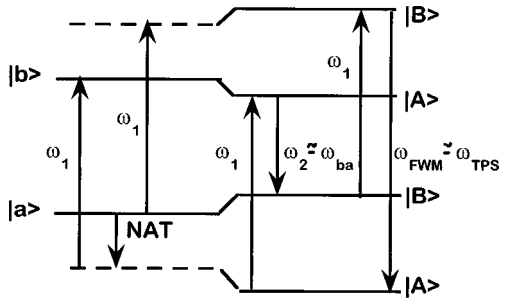

FIG. 8. FWM process. A nonadiabatic transition (NAT) induces population transfer from $|a\rangle$ to $|A\rangle$ so that $|b\rangle$ becomes occupied by absorption of a pump photon allowing the resonance-enhanced $|b\rangle\rightarrow|a\rangle$ transition by a probe photon at $\omega_2\simeq\omega_{ba}$. $|A\rangle$ and $|B\rangle$ are the energetically lower and upper instantaneous semiclassical dressed-atom states [7]. The double use of the dressed-atom states is reminiscent of quantum photon occupation number states. Here classical fields are considered and the quantum photon states are replaced by ''Floquet states'' [15].

near the resonance frequency will be larger than that of the sideband near the TPS frequency for probes with narrow linewidth. The asymmetry will gradually invert as the probe linewidth increases: For a sufficiently large probe linewidth, only the TPS sideband of the FWM excitation spectrum, and hence the resonance sideband in the FWM signal, will survive. These predictions are independent of the way these laser linewidths are varied: whether by changing the durations $D_{1,2}$ of the laser pulses [see Eqs. (19) and (20)] or, in the steady state, by varying $\gamma_{1,2}$ [see Eq. (24)].

When there is a time delay between the pump and probe pulses and the probe pulse is sufficiently short, we predict that the intensity of the Rabi sideband near the resonance frequency strongly varies with the sign of the time delay, whereas the intensity of the TPS sideband remains essentially constant.

APPENDIX

It has been claimed that the adiabaticity condition of Eq. (23) holds for two regimes. The far-detuned, small-signal (large-Δ_1, small-V_1) regime has been fully discussed in this paper. We now discuss the second regime: the near-detuning, large-signal (small-Δ_1, large-V_1) regime.

The adiabatic condition of Eq. (23), for the case of a Gaussian pump [Eq. (19)], can be simplified by making the substitutions

$$\Delta_1 = V_1/a, \quad 1/D_1 = V_1/b. \tag{A1}$$

Then Eq. (23) becomes, after some rearrangement,

$$\frac{a}{b}\frac{|4ax\,\exp(-x^2)|}{[1+4a^2\,\exp(-2x^2)]^{3/2}} = \frac{a}{b}F(a,x) \ll 1, \tag{A2}$$

where the dimensionless variable $x = V_1 t/b$. We now calculate the maximum value $F_{\max}(a,x)$ of $F(a,x)$ as a function of x for various values of $a>1$. Note that increasing a corresponds to decreasing detuning. For $a=1$, 10^2, 10^4, 10^6, 10^8, and 10^{10}, $F_{\max}(a,x) = 0.84$, 1.83, 2.47, 2.97, 3.39, and 3.78, respectively, and the values of x for which the maximum is obtained vary from 1 to 5 as a increases from 1 to 10^{10}.

Let us now consider the validity of the adiabaticity condition, given by Eq. (A2), for the near-detuning, large-signal case. For the large-signal case where

$$V_1 > \Delta_1, \quad a>1, \; F_{\max}(a,x)>1, \tag{A3}$$

the adiabaticity condition holds if

$$\frac{a}{b} = \frac{1}{\Delta_1 D_1} \ll 1 \tag{A4}$$

or

$$\Delta_1 \gg 1/D_1. \tag{A5}$$

This is the same as the first inequality of Eq. (22). For the near-resonance case,

$$\Delta_1 T_2 < 1, \tag{A6}$$

which, combined with Eq. (A5), yields

$$1 > \Delta_1 T_2 \gg T_2/D_1 \tag{A7}$$

and hence

$$1/D_1 \ll 1/T_2. \tag{A8}$$

This implies a long pulse that leads to a symmetrical FWM excitation spectrum as in the steady state. It should be noted that Eq. (A8) is exactly the opposite of the second inequality of Eq. (22)

$$1/D_1 > 1/T_2. \tag{A9}$$

This shows that the near-resonance, large-signal case can never be adiabatic because, if Eq. (A8) holds, transverse relaxation will induce nonadiabatic transitions during the time the pulse interacts with the atoms. The only way to obtain *strongly asymmetrical* spectra in the near-resonance, strong-signal case is to respect the inequality of Eq. (A9) rather than that of Eq. (A8), which derives from the adiabaticity condition, and to allow nonadiabatic transitions.

[1] R. W. Boyd, M. G. Raymer, P. Narum, and D. J. Harter, Phys. Rev. A **24**, 411 (1981).

[2] A. R. Bogdan, Y. Prior, and N. Bloembergen, Opt. Lett. **6**, 82 (1981); A. R. Bogdan, M. W. Downer, and N. Bloembergen, *ibid.* **6**, 348 (1981).

[3] A. D. Wilson-Gordon and H. Friedmann, Phys. Rev. A **38**, 4087 (1988).

[4] W. Chalupczak, W. Gawlik, and J. Zachorowski, Phys. Rev. A **49**, 4895 (1994).

[5] H. Friedmann and A. D. Wilson-Gordon, Phys. Rev. A **36**, 1333 (1987).

[6] A. D. Wilson-Gordon and H. Friedmann, Opt. Lett. **8**, 617 (1983).

[7] P. R. Berman and R. Salomaa, Phys. Rev. A **25**, 2667 (1981); P. R. Berman, *ibid.* **53**, 2627 (1996).

[8] D. Grischkowsky, Phys. Rev. A **14**, 802 (1976).

[9] A. Flushberg and S. R. Hartmann, Phys. Rev. A **14**, 813 (1976).

[10] L. Allen and J. H. Eberly, *Optical Resonance and Two-Level Atoms* (Wiley, New York, 1975).

[11] J. Gea-Banacloche, Y. Li, S. Jin, and M. Xiao, Phys. Rev. A **51**, 576 (1995).

[12] G. S. Agarwal and J. Cooper, Phys. Rev. A **26**, 2761 (1982).

[13] S. Sultana and M. S. Zubairy, Phys. Rev. A **49**, 438 (1994).

[14] A. E. Siegman, *Lasers* (University Science Books, Mill Valley, CA, 1986).

[15] J. H. Shirley, Phys. Rev. **138**, B979 (1965).